# Thermal radiation effect on boundary layer over a flat plate having convective surface boundary condition

Basant K. Jha[1] · Gabriel Samaila[1]

## Abstract

This paper presents the effect of thermal radiation on the boundary layer over a flat plate. The convective boundary condition is applied at the surface of the flat plate. The solution to the coupled non-linear transport equations is obtained using the Runge–Kutta–Fehlberg fourth-fifth order (RKF45) method. The impact of thermal radiation on mercury, air, sulphur oxide and water whose Prandtl numbers (Pr) are 0.044, 0.72, 2, and 7 respectively are depicted using line graphs and tables. The impact of Prandtl number (Pr), local convective heat transfer ($a$) and temperature difference ($C_T$) on temperature distribution are also presented. The results indicated that the boundary layer thickness decreases with Pr augment but increases with increasing values $R$. Furthermore, $R$ augment is inversely proportional to the temperature gradient near the plate while an opposite trend is observed away from the plate. The results also indicated that $R$ augment reduces heat transfer but an opposite trend is observed with Pr augment. Pr augment has a decreasing effect on boundary layer thickness and $a$ augment has an increasing effect on temperature.

## List of symbols

| | |
|---|---|
| $q_r$ | Radiative heat flux |
| $K$ | Thermal conductivity |
| $\psi$ | Stream function |
| $R$ | Thermal radiation parameter |
| $C_T$ | Temperature difference parameter |
| Pr | Prandtl number |
| $\theta$ | Dimensionless temperature |
| Re | Reynolds number |
| $a$ | Local convective heat transfer parameter |

## 1 Introduction

The boundary layer has a wide range of applications ranging from household to engineering practices such as aerodynamics (e.g. in separation and reattachment), species transport (e.g. blowing for cleaning the dust), heat transfer enhancement, mixing enhancement, golf ball aerodynamics etc. The similarity solution for flow and the heat transfer in/over different geometries considering constant surface temperature and convective surface boundary conditions has been reported by [1–5]. These authors demonstrated the possibility for the governing equations to have similarity solutions. Das [6] demonstrated that the plate temperature of a flat plate thermometer is less than one for a fluid whose Prantl number (Pr) is less than one and greater than one for a fluid whose Pr is greater than one. Furthermore, the plate temperature is approximately $Pr^{1/2}$ for Pr close to one. Some of the recent investigations on boundary layer include Khan et al. [7] who analysed the boundary layer flow of a nanofluid over a vertical wall. A comprehensive report on an empirical method of finding a Nusselt number in an enclosure with radiation effect has been present by Hagiwara et al. [8].

✉ Gabriel Samaila, gabbbooooo@yahoo.com; Basant K. Jha, basant777@yahoo.co.uk | [1]Department of Mathematics, Ahmadu Bello University, Zaria, Kaduna, Nigeria.

Thermal radiation is a process by which energy is emitted directly from the radiated surface in the form of an electromagnetic wave in all direction. From the engineering and physical point of view, thermal radiation effect has a pivotal role in the flow of different liquid and heat transfer. Thermal radiation is found to be useful in engineering processes which require high operating temperature. These include; the design of the nuclear plant, gas turbine, aircraft, space vehicle, reliable equipment, satellite etc. Satter and Hamid [9] analysed the significant impact of thermal radiation on unsteady free convection flow in a boundary layer. The role of thermal radiation on free convection boundary layer flow in a vertical parallel has been studied by [10–13]. Thermal radiation on magnetohydrodynamics (MHD) considering different geometries has been addressed [14–18]. These authors demonstrated that the temperature distribution enhanced with thermal radiation. The impact of the thermal radiation on the thermal boundary layer considering different geometry has been studied by [19–21]. The authors concluded that the temperature of the plate is enhanced as thermal radiation magnitude increases. Some recent work on the impact of thermal radiation on the fluid flow considering different geometries includes Cao and Baker [22] who examined heat transfer by radiation on boundary layer through optical fluid past a vertical wall. Aly and Ebaid [23] in their report presented on the role of thermal radiation and suction/injection on boundary layer nanofluid flow over a porous medium considering the induced magnetic field effect concluded that the velocity of the nanofluid flow decreases with volume fraction augment. Hayat et al. [24] also presented the role of radiation in a stagnation point flow of carbon nanofluid considering a stretching cylinder. Ghadikolaei et al. [25] numerically analysed the impact of the thermal radiation on boundary layer past a stretching surface. Tian et al. [26] analysed the significant effect of radiation properties on magnetohydrodynamics (MHD) boundary layer flow past a stretching surface. Shahid et al. [27] numerically analysed the effects of various slip and radiation on unsteady magnetohydrodynamics nanofluid flow past a stretching surface. Ymeli et al. [28] presented an analytic solution of Fourier and radiation conduction in an optical complex medium.

Following the work of Aziz [5], it appeared more appropriate to use convective surface boundary condition instead of the so-called constant surface boundary condition. Furthermore, several works carried out using constant surface boundary condition were revisited using the convective surface boundary condition. Makinde and Aziz [29] presented a report on MHD mixed convection flow from a vertical wall considering the convective boundary condition. Makinde and Olanrewaju [30] analysed the significant effect of thermal buoyancy on the boundary layer over a vertical wall with a convective boundary condition. Yao et al. [31] examined the heat transfer past a stretching/shrinking sheet considering convective surface boundary condition. Aljoufi and Ebaid [32] presented an exact solution of the significant impact of convective boundary condition on the boundary layer slip flow over a stretching surface. Lopez et al. [33] examined the significant role of thermal radiation with convective boundary condition on MHD nanofluid in a microchannel. Hassan and Salawu [34] analysed the convective surface boundary effect on buoyancy-driven flow in a parallel channel.

From the above literature, it is obvious that the impact of thermal radiation on the boundary layer considering convective surface boundary has not been given much attention. Therefore, the overall objective of the present paper is to examine the significant role of thermal radiation on the boundary layer considering a convective surface boundary condition. This is achieved by considering four different fluids namely; mercury, air, sulphur oxide and water, whose Pr are 0.044, 0.72, 2 and 7 respectively.

## 2  Problem statement

Consider the hydrodynamics and boundary layer over a flat plate in the presences of thermal radiation. Let the uniform velocity of the fluid moving on plate surface be $U_\infty$, at the temperature $T_\infty$ as illustrated in Fig. 1. Let $x$ and $y$-axis be along and normal to the flat plate respectively. Then, governing equations can be written as;
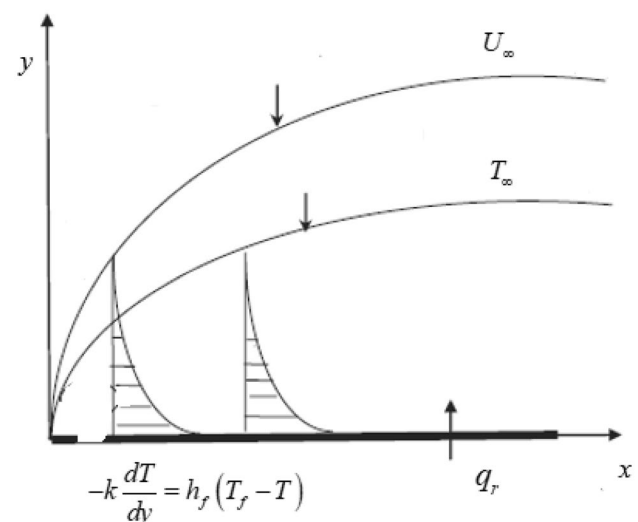


Fig. 1 Flow configuration and coordinate system

$$\frac{\partial u}{\partial x} + \frac{\partial v}{dy} = 0, \tag{1}$$

$$u\frac{\partial u}{\partial x} + v\frac{\partial u}{dy} = v\frac{\partial^2 u}{\partial y^2}, \tag{2}$$

$$u\frac{\partial T}{\partial x} + v\frac{\partial T}{\partial y} = \alpha \left[\frac{\partial^2 T}{\partial y^2} - \frac{1}{K}\frac{\partial q_r}{\partial y}\right], \tag{3}$$

where T denote the dimensional temperature, $K$ denotes the thermal conductivity, $u$ and $v$ denote the velocity component along and normal to the plate. The quantity $q_r$ in Eq. (3) is the radiative heat flux in the y-direction. However, the radiative heat flux in the x-direction is assumed to be small in comparison to that in the y-direction. The radiative heat flux $q_r$ can be simplified through Rosseland diffusion approximation for an optical thick fluid according to [35–39] as

$$q_r = \frac{4\sigma}{3k^*}\frac{\partial T^4}{\partial y}, \tag{4}$$

where $\sigma$ and $k^*$ represent the Stefan Boltzmann constant and mean absorption respectively. Furthermore, Rosseland approximation is only applicable for an optically thick fluid. However, regardless of these limitations, it has been adopted in several investigations ranging from the analysis of radiation effect on blast waves by the nuclear explosion to the transport of radiation through gases at low-density Ali Agha et al. [39].

The velocity boundary conditions can be expressed as

$$u(x, y = 0) = v(x, y = 0) = 0$$
$$u(x, y \to \infty) = U_\infty. \tag{5}$$

Regarding the temperature boundary condition, the base of the plate is assumed to be heated through convection from a hot fluid at a temperature $T_f$ which provides a heat transfer coefficient $h_f$. Therefore, the boundary conditions can be expressed as

$$-k\frac{\partial T}{\partial y}(x, y = 0) = h_f\left[T_f - T(x, y = 0)\right],$$
$$T(x, y \to \infty) = T_\infty. \tag{6}$$

We define the similarity variable $\eta$ and a dimensionless temperature $\theta(\eta)$ and a stream function $f(\eta)$ as

$$\eta = y\sqrt{\frac{U_\infty}{vx}}, \quad u = U_\infty f'(\eta),$$
$$v = \frac{1}{2}\sqrt{\frac{U_\infty v}{x}}\left(\eta f'(\eta) - f\right), \quad \theta = \frac{T - T_\infty}{T_f - T_\infty}.$$

Dimensionless parameters are defined as;

$$\mathrm{Pr} = \frac{\mu C_p}{K}, \tag{7}$$

$$R = \frac{4\sigma(T_f - T_\infty)^3}{k^*K}, \quad C_T = \frac{T_\infty}{T_f - T_\infty}. \tag{8}$$

Finally, the dimensionless equations can be written as;

$$2f'''(\eta) + f(\eta)f''(\eta) = 0, \tag{9}$$

$$\theta''(\eta)\left[1 + \frac{4R}{3}(\theta + C_T)^3\right] + 4R[C_T + \theta]^2[\theta'(\eta)]^2 + \frac{1}{2}\mathrm{Pr}\,\theta'(\eta)f(\eta) = 0. \tag{10}$$

Subject to;

$$f(0) = f'(0) = 0, \quad f'(\eta \to \infty) = 1, \tag{11}$$

$$\theta'(0) = -a[1 - \theta(0)], \quad \theta(\eta \to \infty) = 0, \tag{12}$$

where $C_T$, Pr and $R$ are temperature difference parameter, Prandtl number and thermal Radiation parameter respectively.

We define

$$a = \frac{h_f}{k}\sqrt{\frac{vx}{U_\infty}}. \tag{13}$$

Note that for the energy equation to have a similarity solution, the local convective heat transfer parameter $a$ must be a constant and not function of $x$ as it appeared in Eq. (13). This proposition is feasible if $h_f$ is directly proportional to $x^{-1/2}$. Hence we write

$$h_f = cx^{-1/2}, \tag{14}$$

where $c$ is constant.

Utilizing Eq. (14) in Eq. (13), we have

$$a = \frac{c}{k}\sqrt{\frac{v}{U_\infty}}. \tag{15}$$

Therefore, with $a$ defined in Eq. (15), the solutions of Eqs. (9)–(12), gives the similarity solutions and the sets of solutions generated when $a$ is defined as in Eq. (13) are called the local similarity solutions.

## 3 Results

### 3.1 Discussion

The thermal radiation effect on the thermal boundary layer past a flat plate considering the convective boundary condition is numerically studied. Maple software is used to solve Eqs. (9)–(12) using the RKF45 method.

**Table 1** Comparison of the present results with Aziz [5] for $R=0$ and $C_T=0.2$

| a | Pr = 0.72 | | | | Pr = 10 | | | |
|---|---|---|---|---|---|---|---|---|
| | $\theta(0)$ | | $-\theta'(0)$ | | $\theta(0)$ | | $-\theta'(0)$ | |
| | Aziz [5] | Present work | Aziz [5] | Present work | Aziz [5] | Present work | Aziz [5] | Present work |
| 0.05 | 0.1447 | 0.1447 | 0.0428 | 0.0428 | 0.0643 | 0.0643 | 0.0468 | 0.0468 |
| 0.10 | 0.2528 | 0.2528 | 0.0747 | 0.0747 | 0.1208 | 0.1208 | 0.0879 | 0.0879 |
| 0.20 | 0.4035 | 0.4035 | 0.1193 | 0.1193 | 0.2155 | 0.2155 | 0.1569 | 0.1569 |
| 0.40 | 0.5750 | 0.5750 | 0.1700 | 0.1700 | 0.3546 | 0.3546 | 0.2582 | 0.2582 |
| 0.60 | 0.6699 | 0.6699 | 0.1981 | 0.1981 | 0.4518 | 0.4518 | 0.3289 | 0.3298 |
| 0.80 | 0.7302 | 0.7302 | 0.2159 | 0.2159 | 0.5235 | 0.5235 | 0.3812 | 0.3812 |
| 1 | 0.7717 | 0.7717 | 0.2282 | 0.2282 | 0.5787 | 0.5787 | 0.4213 | 0.4213 |
| 5 | 0.9441 | 0.9441 | 0.2791 | 0.2791 | 0.8729 | 0.8729 | 0.6356 | 0.6356 |
| 10 | 0.9713 | 0.9713 | 0.2871 | 0.2871 | 0.9321 | 0.9321 | 0.6787 | 0.6787 |
| 20 | 0.9854 | 0.9854 | 0.2913 | 0.2913 | 0.9649 | 0.9649 | 0.7026 | 0.7026 |

**Table 2** Comparison of the present results with Makinde [30] for Pr = 0.72, $R=0$ and $C_T=0.2$

| a | $\theta(0)$ | | $-\theta'(0)$ | |
|---|---|---|---|---|
| | Makinde and Olanrewaju [30] | Present work | Makinde and Olanrewaju [30] | Present work |
| 0.05 | 0.1447 | 0.1447 | 0.0428 | 0.0428 |
| 0.10 | 0.2528 | 0.2528 | 0.0747 | 0.0747 |
| 0.20 | 0.4035 | 0.4035 | 0.1193 | 0.1193 |
| 0.40 | 0.5750 | 0.5750 | 0.1700 | 0.1700 |
| 0.60 | 0.6699 | 0.6699 | 0.1981 | 0.1981 |
| 0.80 | 0.7302 | 0.7302 | 0.2159 | 0.2159 |
| 1 | 0.7717 | 0.7717 | 0.2282 | 0.2282 |
| 5 | 0.9441 | 0.9441 | 0.2791 | 0.2791 |
| 10 | 0.9713 | 0.9713 | 0.2871 | 0.2871 |
| 20 | 0.9854 | 0.9854 | 0.2913 | 0.2913 |
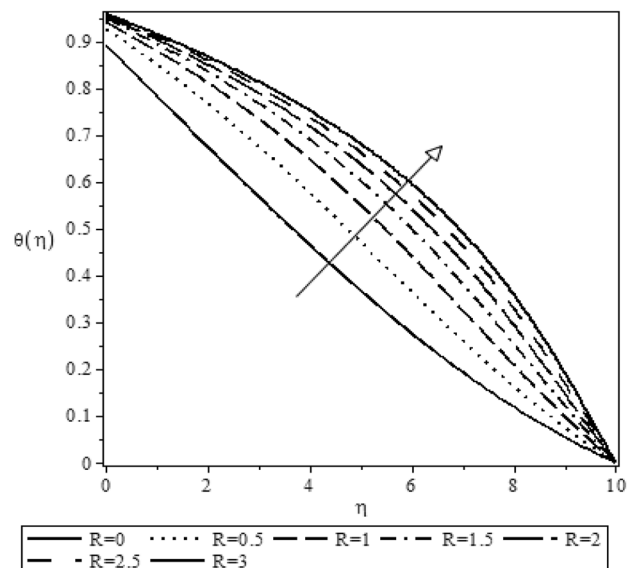


**Fig. 2** Impact of $R$ variation on temperature distribution for mercury fluid ($a = 1$, $C_T = 0.2$)

RKF45 is a default method in Maple due to its accuracy and robustness. Four different fluids considered are mercury, air, sulphur oxide and water whose Prandtl number (Pr) are 0.044, 0.72, 2 and 7 respectively. It is found that the solution converged when $\eta \to 10$, hence $\infty$ is replaced by 10 throughout the computation. The thermal radiation parameter ($R$) used are 0, 0.5, 1, 1.5, 2, 2.5, 3, 3.5 and 4. The local convective heat transfer parameter ($a$) used in the present numerical computation are 0.05, 0.10, 0.20, 0.40, 0.60, 0.80, 1, 5, 10, and 20. Also, the temperature difference parameter ($C_T$) used are 0, 0.2, 0.4, 0.6, 0.8 and 1. The present study is validated through comparison with Aziz [5] and Makinde and Olanrewaju [30]. Table 1 and Table 2 demonstrates the accuracy of the present solution of fluid whose Prandtl numbers are 0.72 and 10 for some selected values of $a$ and it is

observed that there is an excellent agreement in the absence of thermal radiation parameter ($R$).

Figures 2, 3, 4 and 5 depict the temperature distribution of mercury, air, sulphur oxide and water for $a = 1$ and $C_T = 0.2$ with various values of $R$. It is evident that the temperature variation is proportional to $R$ for all fluids under consideration. Figure 6 depicts the variation of temperature gradient for different values of $R$ and fixed values of Pr, $a$ and $C_T$. This figure reveals that the temperature gradient of the fluid is inversely proportional to the $R$ near the plate while the impact of the $R$ is just reverse far away from the plate. Furthermore, an increase in Pr decreases boundary layer thickness as depicted in Fig. 7. In general, when Pr is unity, it means that the thermal and momentum diffusion
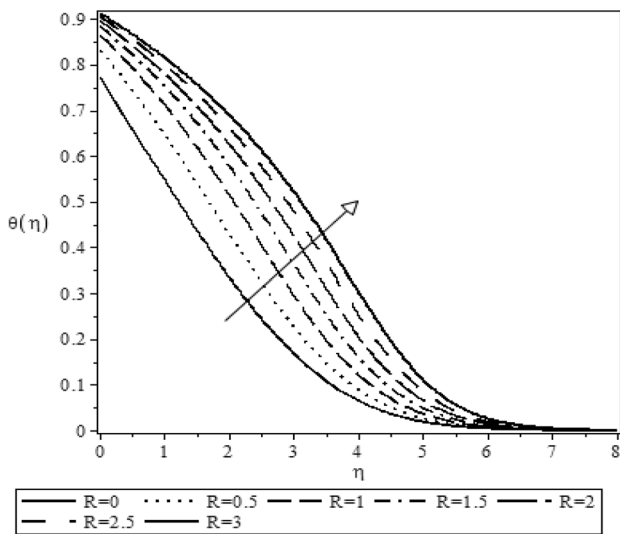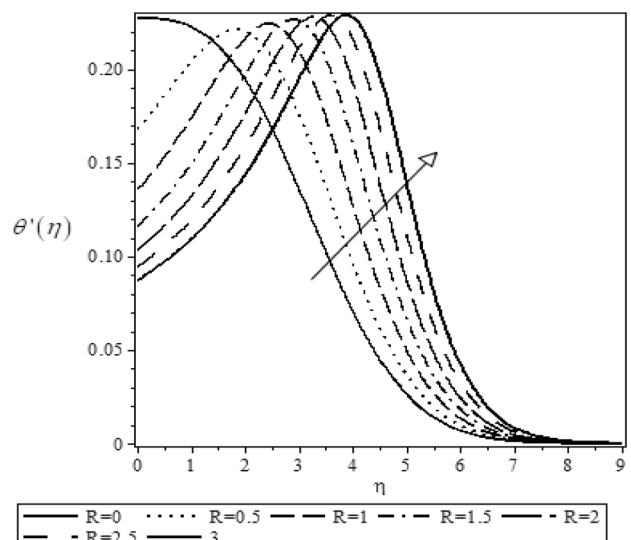
**Fig. 3** Impact of $R$ variation on temperature distribution for air fluid ($a = 1$, $C_T = 0.2$)
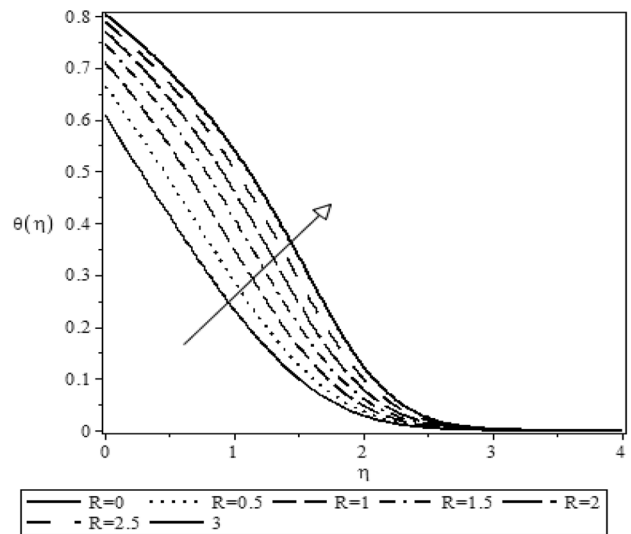


**Fig. 5** Impact of $R$ variation on temperature distribution for water fluid ($a = 1$, $C_T = 0.2$)
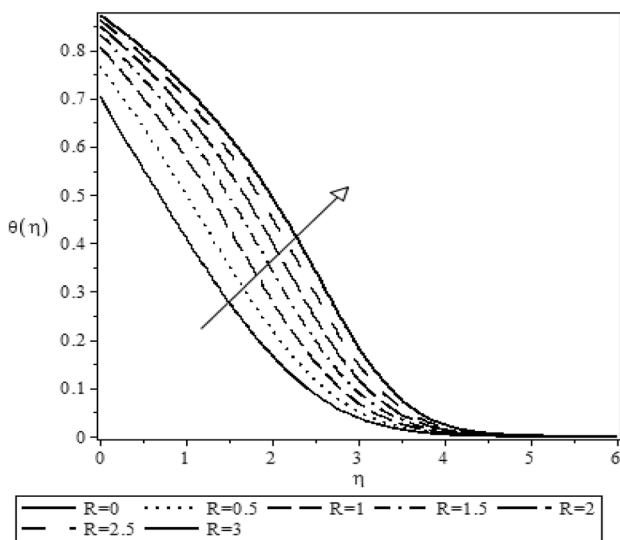


**Fig. 4** Impact of $R$ variation on temperature distribution for sulphur oxide fluid ($a = 1$, $C_T = 0.2$)



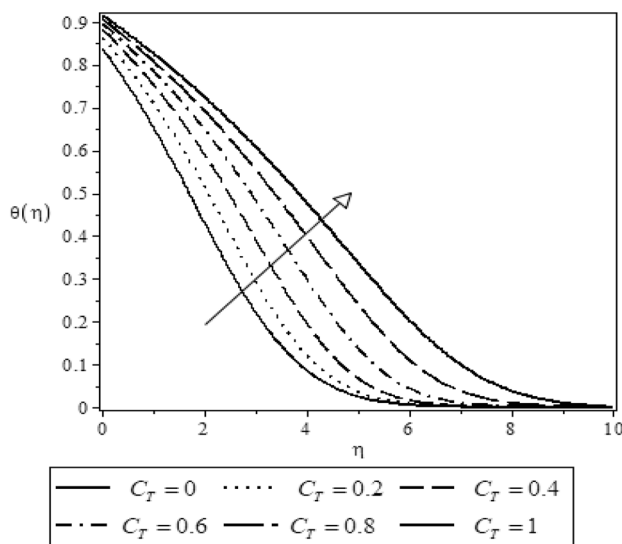**Fig. 6** Impact of $R$ variation on temperature gradient for air fluid ($a = 1, C_T = 0.2$)

are the same order of magnitude, which connote that the thermal and momentum boundary layer overlaps each other. Additionally, for Pr < 1, the thermal diffusivity is higher than viscous diffusivity which means, that the thermal boundary layer is thicker than the momentum boundary layer while the physical situation is just contrasted for Pr > 1. This can be observed in Fig. 7 where mercury has the largest thermal boundary layer thickness while water has the least thermal boundary layer thickness. Figure 8 illustrates the influence of temperature differences parameter ($C_T$) on the temperature distribution for air for fixed

values of $a$ and $R$. It is obvious from the figure that $C_T$ plays a supporting role for temperature distribution. The role of the local convective heat transfer ($a$) is depicted in Fig. 9. It is obvious from the figure that increasing $a$, leads to an increase in the plate surface temperature. The numerical solution of the present work approaches the solution for constant temperature as $a \to \infty$. This follows from Eq. (12) that the boundary condition reduces to $\theta(0) = 1$ as $a \to \infty$.

Table 3 demonstrates the significant effect of $R$ on the surface temperature of the four fluids under consideration. The values of $\theta(0)$ (plate temperature) enhance with $R$ for
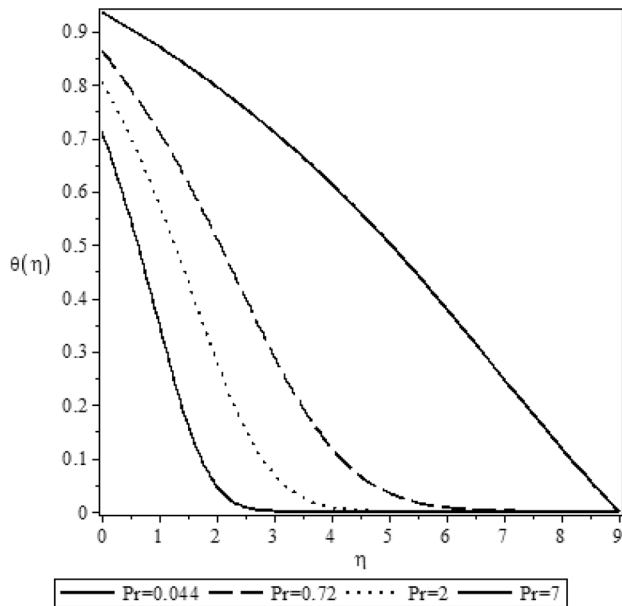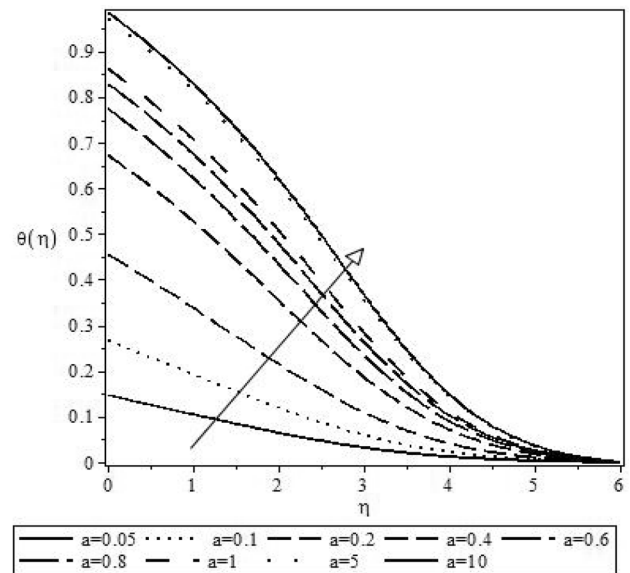
**Fig. 7** Variation of Pr on the boundary layer for $(R=1, a=1)$



**Fig. 9** Variation of $a$ on the temperature distribution for air fluid $(R=1, C_T=0.2)$



**Fig. 8** Variation of $C_T$ on the temperature distribution for air fluid $(R=1, a=1)$

all the four fluids under consideration while the opposite pattern is noticed for $-\theta'(0)$. It can also be seen that as Pr increases, the numerical values of $\theta(0)$ decreases while the numerical value of $-\theta'(0)$ increases. Table 4 shows the effect of grid refinement on $\theta(0)$ with $R$ variation. It can be observed that the numerical values of $\theta(0)$ increases with grid refinement until $\eta$ approaches 10. This shows the

validity for replacement of $\eta \to \infty$ by $\eta = 10$ in the present numerical computation which conforms with the customary practice in boundary layer theory.

## 4 Conclusion

The numerical solution for impact of thermal radiation on thermal boundary layer formation on the flat plate with a convective boundary condition is discussed. The effects of $R, C_T, a$ and Pr on temperature is analysed using line graphs and tables. The results indicated that:

(i) Thermal radiation ($R$) has an increasing effect on the thermal boundary layer thickness and numerical values of $\theta(0)$ while reverse impact on the temperature gradient $-\theta'(0)$.

(ii) The thermal boundary layer thickness decreases as Pr increase.

(iii) As temperature differences increases ($C_T$), the temperature distribution increases.

(iv) The numerical solution approaches contant surface temperature solution as $a \to \infty$.

(v) The temperature distribution enhanced with $a$ augment.

**Table 3** Effect of R on $\theta(0)$ and $-\theta'(0)$ for $a=1$ and $C_T = 0.2$

| R | Pr = 0.044 | | Pr = 0.72 | | Pr = 2 | | Pr = 7 | |
|---|---|---|---|---|---|---|---|---|
| | $\theta(0)$ | $-\theta'(0)$ | $\theta(0)$ | $-\theta'(0)$ | $\theta(0)$ | $-\theta'(0)$ | $\theta(0)$ | $-\theta'(0)$ |
| 0.0 | 0.8915 | 0.1085 | 0.7729 | 0.2273 | 0.7031 | 0.2969 | 0.6076 | 0.3924 |
| 0.5 | 0.9276 | 0.0723 | 0.8324 | 0.1676 | 0.7661 | 0.2339 | 0.6648 | 0.3352 |
| 1.0 | 0.9419 | 0.0581 | 0.8648 | 0.1352 | 0.8068 | 0.1932 | 0.7113 | 0.2887 |
| 1.5 | 0.9492 | 0.0508 | 0.8840 | 0.1660 | 0.8327 | 0.1673 | 0.7456 | 0.2543 |
| 2.0 | 0.9537 | 0.0463 | 0.8967 | 0.1033 | 0.8502 | 0.1498 | 0.7706 | 0.2294 |
| 2.5 | 0.9567 | 0.0433 | 0.9057 | 0.0943 | 0.8630 | 0.1370 | 0.7893 | 0.2107 |
| 3.0 | 0.9588 | 0.0412 | 0.9126 | 0.0874 | 0.8727 | 0.1273 | 0.8038 | 0.1932 |
| 3.5 | 0.9604 | 0.0396 | 0.9181 | 0.0819 | 0.8803 | 0.1197 | 0.8154 | 0.1846 |
| 4 | 0.9616 | 0.0384 | 0.9226 | 0.0774 | 0.8866 | 0.1134 | 0.8248 | 0.1752 |

**Table 4** Grid independency on $\theta(0)$ for Pr = 0.72, $a=1$ and $C_T = 0.2$

| R | $\eta = 1$ | $\eta = 2$ | $\eta = 3$ | $\eta = 4$ | $\eta = 6$ | $\eta = 8$ | $\eta = 9$ | $\eta = 10$ |
|---|---|---|---|---|---|---|---|---|
| 0.0 | 0.4962 | 0.6527 | 0.7219 | 0.7540 | 0.7709 | 0.7718 | 0.7718 | 0.7718 |
| 0.5 | 0.5332 | 0.7098 | 0.7818 | 0.8138 | 0.8306 | 0.8316 | 0.8316 | 0.8316 |
| 1.0 | 0.5681 | 0.7496 | 0.8173 | 0.8470 | 0.8631 | 0.8641 | 0.8641 | 0.8641 |
| 1.5 | 0.5983 | 0.7755 | 0.8356 | 0.8665 | 0.8823 | 0.8833 | 0.8833 | 0.8833 |
| 2.0 | 0.6227 | 0.7927 | 0.8522 | 0.8789 | 0.8949 | 0.8961 | 0.8961 | 0.8961 |

## Compliance with ethical standards

## References

1. Ishak A (2010) Similarity solutions for flow and heat transfer over a permeable surface with convective boundary condition. Appl Math Comput 217:837–842
2. Bataller RC (2008) Similarity solutions for flow and heat transfer of a quiescent fluid over a nonlinearly stretching surface. J Mater Process Technol 203(1–3):176–183
3. Makinde OD, Aziz A (2011) Boundary layer flow of a nanofluid past a stretching sheet with a convective boundary condition. Int J Therm Sci 50(7):1326–1332
4. Ishak A, Yacob NA, Bachok N (2011) Radiation effects on the thermal boundary layer flow over a moving plate with convective boundary condition. Meccanica 46(4):795–801
5. Aziz A (2009) A similarity solution for laminar thermal boundary layer over a flat plate with a convective surface boundary condition. Commun Nonlinear Sci Numer Simul 14(4):1064–1068
6. Das K (2012) Impact of thermal radiation on MHD slip flow over a flat plate with variable fluid properties. Heat Mass Transf 48(5):767–778
7. Khan WA, Makinde OD, Khan ZH (2014) MHD boundary layer flow of a nanofluid containing gyrotactic microorganisms past a vertical plate with Navier slip. Int J Heat Mass Transf 74:285–291
8. Hagiwara I, Tokuhiro A, Oduor PG (2020) Empirical derivation of a Nusselt number in a thermally stratified enclosure. Int J Therm Sci 149:106209
9. Sattar MDA, Kalim H (1996) Unsteady free-convection interaction with thermal radiation in a boundary layer flow past a vertical porous plate. J Math Phys Sci 30(1):25–37
10. Hossain MA, Takhar HS (1996) Radiation effect on mixed convection along a vertical plate with uniform surface temperature. Heat Mass Transf 31(4):243–248
11. Raptis A (1998) Radiation and free convection flow through a porous medium. Int Commun Heat Mass Transf 25(2):289–295
12. El-Hakiem MA (2000) MHD oscillatory flow on free convection–radiation through a porous medium with constant suction velocity. J Magn Magn Mater 220(2–3):271–276
13. Makinde OD (2005) Free convection flow with thermal radiation and mass transfer past a moving vertical porous plate. Int Commun Heat Mass Transf 32(10):1411–1419
14. Mahmoud MAA (2007) Thermal radiation effects on MHD flow of a micropolar fluid over a stretching surface with variable thermal conductivity. Phys A Stat Mech Appl 375(2):401–410
15. Ibrahim FS, Elaiw AM, Bakr AA (2008) Effect of the chemical reaction and radiation absorption on the unsteady MHD free convection flow past a semi infinite vertical permeable moving plate with heat source and suction. Commun Nonlinear Sci Numer Simul 13(6):1056–1066
16. Suneetha S, Bhaskar Reddy N, Ramachandra Prasad V (2008) Thermal radiation effects on MHD free convection flow past an impulsively started vertical plate with variable surface temperature and concentration. J Nav Arch Mar Eng 5(2):57–70
17. Das K, Sarkar A (2016) Effect of melting on an MHD micropolar fluid flow toward a shrinking sheet with thermal radiation. J Appl Mech Tech Phys 57(4):681–689
18. Waqas M, Khan MI, Hayat T, Alsaedi A (2017) Numerical simulation for magneto Carreau nanofluid model with thermal radiation: a revised model. Comput Methods Appl Mech Eng 324:640–653

19. Makinde OD, Ogulu A (2008) The effect of thermal radiation on the heat and mass transfer flow of a variable viscosity fluid past a vertical porous plate permeated by a transverse magnetic field. Chem Eng Commun 195(12):1575–1584

20. Bhattacharyya K, Layek GC (2011) Effects of suction/blowing on steady boundary layer stagnation-point flow and heat transfer towards a shrinking sheet with thermal radiation. Int J Heat Mass Transf 54(1):302–307

21. Ishak A (2011) MHD boundary layer flow due to an exponentially stretching sheet with radiation effect. Sains Malays 40(4):391–395

22. Cao K, Baker J (2015) Non-continuum effects on natural convection–radiation boundary layer flow from a heated vertical plate. Int J Heat Mass Transf 90:26–33

23. Aly EH, Ebaid A (2016) Exact analysis for the effect of heat transfer on MHD and radiation Marangoni boundary layer nanofluid flow past a surface embedded in a porous medium. J Mol Liq 215:625–639

24. Hayat T, Khan MI, Waqas M, Alsaedi A, Farooq M (2017) Numerical simulation for melting heat transfer and radiation effects in stagnation point flow of carbon–water nanofluid. Comput Methods Appl Mech Eng 315:1011–1024

25. Ghadikolaei SS, Hosseinzadeh K, Yassari M, Sadeghi H, Ganji DD (2017) Boundary layer analysis of micropolar dusty fluid with $TiO_2$ nanoparticles in a porous medium under the effect of magnetic field and thermal radiation over a stretching sheet. J Mol Liq 244:374–389

26. Tian X-Y, Li B-W, Zhang J-K (2017) The effects of radiation optical properties on the unsteady 2D boundary layer MHD flow and heat transfer over a stretching plate. Int J Heat Mass Transf 105:109–123

27. Khan SA, Nie Y, Ali B (2019) Multiple slip effects on MHD unsteady viscoelastic nano-fluid flow over a permeable stretching sheet with radiation using the finite element method. SN Appl Sci 2(1):66

28. Ymeli GL, Kamdem HTT, Tchinda R, Lazard M (2019) Analytical layered solution of radiation and non-Fourier conduction problems in optically complex media. Int J Heat Mass Transf 145:118712

29. Makinde OD, Aziz A (2010) MHD mixed convection from a vertical plate embedded in a porous medium with a convective boundary condition. Int J Therm Sci 49(9):1813–1820

30. Makinde OD, Olanrewaju PO (2010) Buoyancy effects on thermal boundary layer over a vertical plate with a convective surface boundary condition. J Fluids Eng 132(4):44502

31. Yao S, Fang T, Zhong Y (2011) Heat transfer of a generalized stretching/shrinking wall problem with convective boundary conditions. Commun Nonlinear Sci Numer Simul 16(2):752–760

32. Aljoufi MD, Ebaid A (2016) Effect of a convective boundary condition on boundary layer slip flow and heat transfer over a stretching sheet in view of the exact solution. J Theor Appl Mech 46(4):85–95

33. Lopez A, Ibanez G, Pantoja J, Moreira J, Lastres O (2017) Entropy generation analysis of MHD nanofluid flow in a porous vertical microchannel with nonlinear thermal radiation, slip flow and convective–radiative boundary conditions. Int J Heat Mass Transf 107:982–994

34. Hassan AR, Salawu SO (2019) Analysis of buoyancy driven flow of a reactive heat generating third grade fluid in a parallel channel having convective boundary conditions. SN Appl Sci 1(8):919

35. Jha BK, Isah BY, Uwanta IJ (2016) Combined effect of suction/injection on MHD free-convection flow in a vertical channel with thermal radiation. Ain Shams Eng J 9:1069–1088

36. Hossain MA, Alim MA, Rees DAS (1999) The effect of radiation on free convection from a porous vertical plate. Int J Heat Mass Transf 42(1):181–191

37. Aydın O, Kaya A (2009) MHD mixed convective heat transfer flow about an inclined plate. Heat Mass Transf 46(1):129

38. Rashad AM (2009) Perturbation analysis of radiative effect on free convection flows in porous medium in the presence of pressure work and viscous dissipation. Commun Nonlinear Sci Numer Simul 14(1):140–153

39. Ali Agha H, Bouaziz MN, Hanini S (2014) Free convection boundary layer flow from a vertical flat plate embedded in a Darcy porous medium filled with a nanofluid: effects of magnetic field and thermal radiation. Arab J Sci Eng 39(11):8331–8340